

AD-A098 18*

KANSAS STATE UNIV MANHATTAN DEPT OF PHYSICS
TIME-RESOLVED RAMAN SCATTERING AND TRANSMISSION MEASUREMENTS DU--ETC(U)
1980 A COMPAAN, H W LO, A AYDINLI, M C LEE N00014-80-C-0419

F/G 20/6

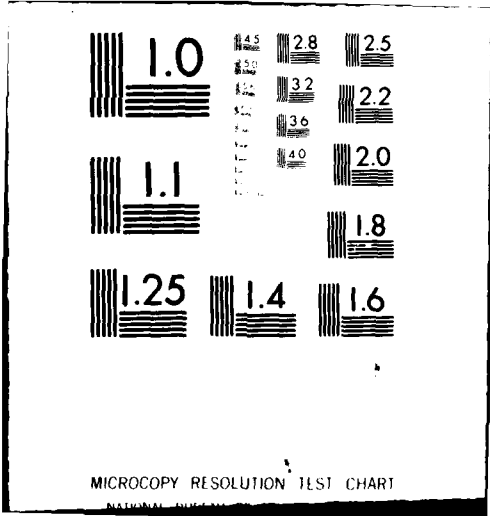
UNCLASSIFIED

NL

(of)
5/8/83



END
DNL
FILMED
5-81
DTIC



TIME-RESOLVED RAMAN SCATTERING AND TRANSMISSION MEASUREMENTS DURING PULSED LASER ANNEALING.

MRS. [unclear] [unclear] 480
(11) 1978
(12)

10 A. /COMPAN, H. W. /LO, A. /AYDINLI, M. C. /LEE
Department of Physics, Kansas State University, Manhattan, Kansas, 66506.

ABSTRACT

Raman scattering from a 7 nsec pulsed dye laser has been used to determine the onset of recrystallization following an 8 nsec dye laser excitation pulse in ion-implanted silicon. We find essentially complete recrystallization 59 nsec after the first excitation pulse and from Stokes-anti-Stokes ratios we find at 59 nsec a crystalline lattice temperature of $600 \pm 200^\circ\text{C}$. Time-resolved transmission measurements at $\lambda = 1.15 \mu\text{m}$ also demonstrate that no molten phase has occurred even though the usual reflectivity enhancement is observed.

DTIC
APR 24 1981

AD A 098184

(13) NC 14-12-1-0429

Laser annealed semiconductors have been studied with a great variety of probes to determine anneal characteristics¹ and the results used to construct scenarios of the anneal process. However, to distinguish between a model which requires thermal melting² and (e.g.) a plasma annealing model³ which predicts little lattice heating, it is highly desirable to acquire time-resolved information of the semiconductor conditions during pulsed annealing. We shall show here that the only time-resolved technique used to date, namely optical reflectivity,^{4,5} has been widely abused as a proof of transient thermal melting of silicon. We report here the first time-resolved phonon Raman measurements of pulsed laser annealing which identify the onset of recrystallization⁶ and give the lattice temperature of the newly recrystallized material. These measurements show that the lattice must remain far below melting during the annealing. Furthermore we present time-resolved reflectivity and transmission measurements at $1.15 \mu\text{m}$ which demonstrate, in agreement with the Raman results, that the high reflectivity phase cannot be molten silicon.

7777

The experimental apparatus, shown in figure 1, includes several important features. 1) A 2.55 meter confocal spherical-mirror delay line was used to obtain adjustable delays for the probe pulse at 406.5 nm . 2) A computer-controlled x-y scanning stage was used to raster-scan the sample to present virgin unannealed surface to each successive laser pulse. 3) A PARC OMA-2 vidicon was used at the output of the Spex 1401 spectrometer for signal detection. 4) All three laser beams were focussed to the same spot through the use of a $50 \mu\text{m}$ pinhole which replaced the sample. 5) The $58 \text{ mm } f/1.4$ collection lens was used with a magnification of 5 to match the spectrometer collection optics. A PDP 11/34 computer controlled the vidicon as well as the sample scanning stage. The OMA-2 was cooled to dry ice temperature and signal was typically integrated for 10 minutes. During readout 10 adjacent channels were integrated before digitizing and then sent to the computer for storage and background subtraction. The effective detector resolution was therefore $250 \mu\text{m}$; however, the image size of $\sim 700 \mu\text{m}$ at the entrance slit was the resolution-limiting factor. To reduce stray light the intermediate slit was typically operated at $1500 \mu\text{m}$.

DTIC FILE COPY

DISTRIBUTION STATEMENT A
Approved for public release;
Distribution Unlimited

403532

1

81 3 05 049

Accession For	
NTIS GRA&I	<input checked="" type="checkbox"/>
DTIC TAB	<input type="checkbox"/>
Unannounced	<input type="checkbox"/>
Justification	
By _____	
Distribution/	
Availability Codes	
Dist	Avail and/or Special
A	

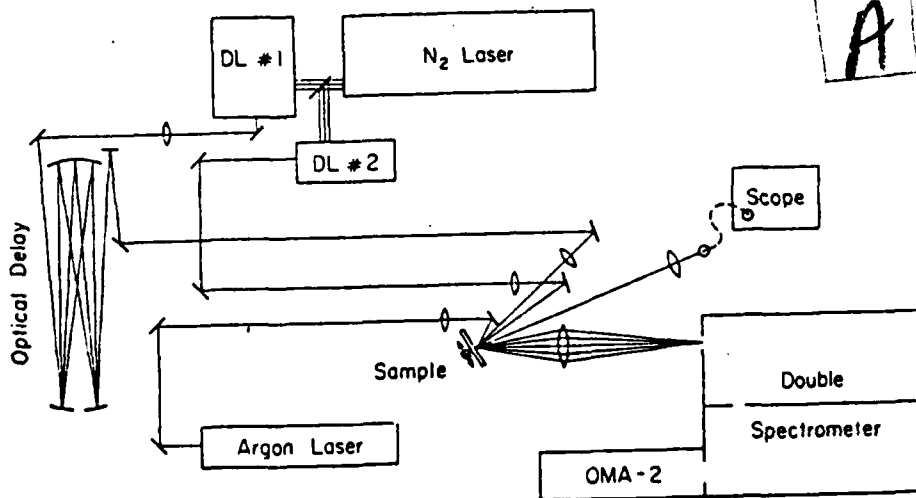


Fig. 1. Experimental apparatus.

The heat/probe technique used a two-beam configuration with an intense annealing beam and a weak, delayed probe beam.⁷ In addition the probe was focussed to a diameter at half power points approximately 1/3 less than the annealing beam which was typically 200 μm . Spot overlap was repeatedly checked with the 50 μm pinhole placed at the exact position of the silicon sample. A Molectron UV-1000 pulsed nitrogen laser operating at 15 Hz was used to excite simultaneously the two dye lasers. Maximum power for the annealing pulse at $\lambda = 485 \text{ nm}$ was obtained from a broad-band dye laser ($\Delta\lambda \approx 10 \text{ nm}$) with no dispersive element in the cavity while the probe pulse at $\lambda = 406.5 \text{ nm}$ was obtained from a Molectron DL-200 dye laser. Note that if some probe light overlaps with the weak fringes of the anneal pulse spot no Raman signal will arise from these regions if no recrystallization has occurred since the spectrum of amorphous silicon is weaker by more than a factor of 100 in the region of 500 cm^{-1} .

The ion-implanted silicon samples were obtained from Spire Corporation implanted with 200 keV arsenic to a dose of $10^{15}/\text{cm}^2$. The projected range of 200 keV arsenic is $0.11 \mu\text{m}$ ⁸ with heavy damage extending somewhat further. A probe pulse at 406.5 nm has an absorption length in room temperature crystalline silicon of $\sim 0.16 \mu\text{m}$ and since the Raman light is absorbed on the way out at nearly the same rate, the effective probe depth is $\sim 0.08 \mu\text{m}$. Higher crystalline temperatures will reduce this depth still further. Thus even if recrystallization has proceeded through to the undamaged substrate, the probe pulse will sample only material originally amorphized by ion-implantation. CW Raman polarization measurements obtained after a single anneal pulse show that the central $\sim 50 \mu\text{m}$ of the annealed spot is oriented exactly as the substrate. TEM measurements⁹ confirm epitaxial regrowth of the central region.

The onset of recrystallization in the ion-implanted amorphized silicon samples was studied using a variety of time delays with the optical delay line. Figure 2 displays Raman signals obtained with an annealing pulse power density of $0.6 \text{ J}/\text{cm}^2$ in the central $50 \mu\text{m}$ and at various probe delays. Clearly the growth of the Raman signal is very rapid. The crystalline signal is essentially full size at 59 nsec and a sizeable signal occurs already at 28 nsec. For comparison we display in the inset the shape of the reflectivity rise observed in this material with a CW 514.5 nm beam focussed to $\sim 40 \mu\text{m}$ diameter at the center of the pulsed beams. The lower trace of the inset shows the two pulsed beams indicating that for some of the duration of the probe pulse at 28 nsec the sample is still in a slightly enhanced reflectivity state.

To examine less ambiguously whether a crystalline signal exists during the high reflectivity phase, we repeated the 28 nsec measurement using a power density of $0.9 \text{ J}/\text{cm}^2$ for the heating pulse. This produced a high reflectivity phase lasting 60 nsec followed by a ~ 25 nsec tail. Amplitude stability of the annealing pulse was $\pm 5\%$ and the reflectivity duration varied by less than $\pm 20\text{ns}$ during data acquisition. The Raman signal was clearly present at a level of ~ 500 counts in 5 minutes. During the high reflectivity phase the reflectivity rises from $\sim 35\%$ to $\sim 60\%$. Since this affects the transmission of scattered light through the surface as well as the laser light, one expects a decrease of $(.4/.65)^2 = .38$ in the Raman signal. This factor can account essentially for all of the drop in signal observed at 28 nsec. This suggests that a Raman signal is present during the high reflectivity phase. However, since the CW reflectivity probe samples only the center $\sim 50 \mu\text{m}$ whereas the Raman probe samples a diameter of $\sim 120 \mu\text{m}$ it is possible that recrystallization begins on the fringes of the anneal area before the enhanced reflectivity phase has decayed in the center. Thus a definitive conclusion on whether the high reflectivity phase may have a crystalline-like Raman signature must await further experiments.

When the Stokes Raman signal has grown to full strength it is possible to obtain a clear anti-Stokes peak as well. This permits a direct measurement of lattice temperature in the newly recrystallized material. This measurement was obtained with a probe delay of 59 ns and annealing pulse power density of $0.6 \text{ J}/\text{cm}^2$. The Stokes-anti-Stokes ratio, using only the discrete feature at $\pm 500 \text{ cm}^{-1}$ in the Raman spectra, indicates a lattice temperature of $600^\circ \pm 200^\circ\text{C}$. Again if a molten phase is required for annealing the crystal temperature should have reached 1400°C . Thus this low lattice temperature, measured only 20 nsec after the recovery of the reflectivity signal, contradicts the hypothesis of thermal melting.

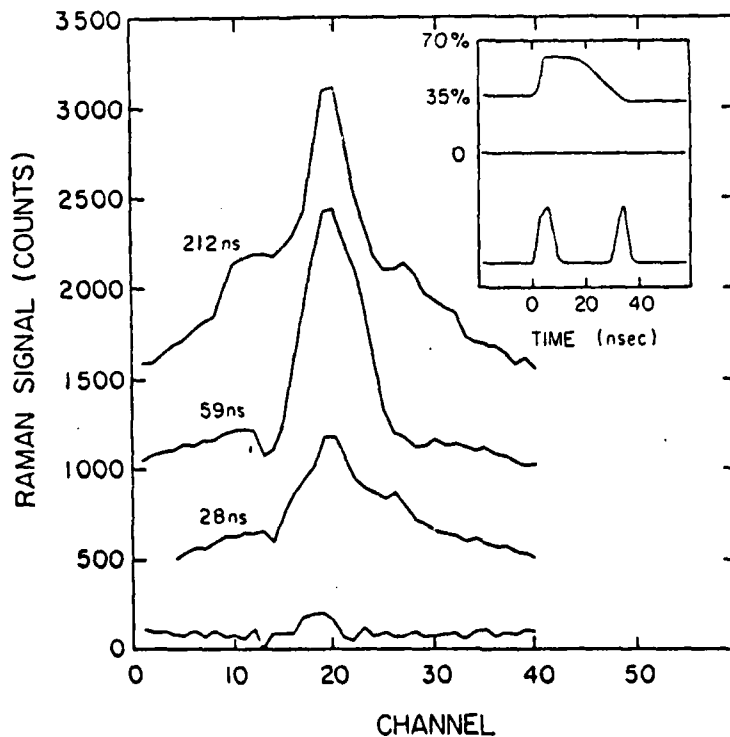


Fig. 2. Stokes Raman spectra of ion-implanted silicon obtained for several probe delays. The lowest trace was taken with the heat beam blocked; successive traces are displaced vertically by 500 counts. Dispersion is $8 \text{ cm}^{-1}/\text{channel}$. Insets show reflectivity at 514 nm and pulse timing at 28 nsec.

In order to extract a lattice temperature from the Stokes-anti-Stokes ratios, it is necessary to correct for differing absorption of the two scattered beams and also for the difference in Raman cross section for the Stokes and anti-Stokes processes.⁷ For these corrections we have used measured values for room temperature crystalline silicon. These corrections are small and not strongly dependent on temperature. However, in the presence of a dense laser-generated electron-hole plasma the electronic properties of the crystal may be changed. Furthermore if the Raman temperature measurements are correct then the interpretation of the enhanced reflectivity signal as proof of a molten phase certainly needs corroboration. Thus, in order to improve our confidence in the absorption corrections to the Raman data and in

order better to understand the origin of the reflectivity enhancement itself we have performed the experiment complementary to reflectivity, *viz.* to measure the time-resolved transmission of this enhanced-reflectivity phase. For the transmission measurements the arrangement of figure 1 was used with the argon laser replaced by a helium-neon laser operating at 1.15 μm . In addition the full N_2 laser power was used to pump the 485 nm dye laser. A measure of relative spot sizes is given by the fraction of power transmitted through the 50 μm pinhole placed at the sample position. For the transmission measurements, greater than 75% of the 1.15 μm beam was transmitted but only 3% of the 485 nm excitation pulse. The time resolved measurements were performed on a 400 μm thick crystalline silicon wafer with the 1.15 μm beam incident at 10° to the normal using a germanium p-i-n detector with a rise time of 3-4 nsec.

The penetration depth of the 485 nm pulsed beam is $\alpha^{-1} = 1.1 \mu\text{m}$ so that if thermal melting occurs one should expect the melt depth at $\sim 1 \text{ J/cm}^2$ to be approximately 1 μm . However if one assumes that only 0.1 μm has melted then the 120 \AA skin depth of molten silicon still requires that the transmission at $\lambda = 1 \mu\text{m}$ would be $e^{-8.3}$. Transmission and reflectivity at 1.15 μm with pulsed beam power of 1 J/cm^2 are shown in figure 3. The transmission shows a sudden drop as the reflectivity rises and a corresponding recovery as the reflectivity falls. It is immediately apparent that the transmission minimum does not in any way approach the $e^{-8.3}$ expected on the basis of the conservative estimate of melt depth given above. This result stands in direct contradiction to the normal thermal melting hypothesis.

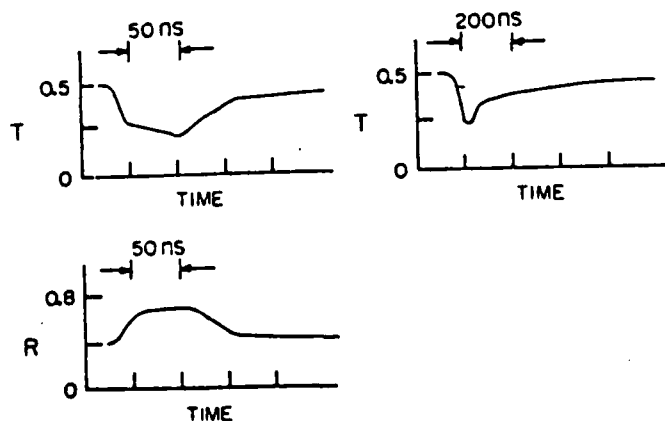


Fig. 3. Transmission and reflectivity of 0.4 mm thick crystalline silicon measured with a CW 1.15 μm probe and a 485 nm excitation pulse.

The sharp drop and recovery in transmission is explained almost entirely by the reflectivity behavior, however the transmission does not fully recover when the reflectivity does. A residual transmission loss of $\pm 30\%$ recovers with a time constant of ~ 400 nsec. We believe this transmission loss may arise from absorption due to free carriers generated by the 485 nm pulse. The absorption corresponds to $\alpha l = 0.35$ where l is the depth of the absorbing region ($l \approx 1 \mu\text{m}$, the pulsed laser absorption depth). Free carrier absorption in silicon due to photogenerated carriers has been measured using a 1.06 μm excitation pulse.¹⁰ The absorption cross section per electron-hole pair at $\sim 1.5 \mu\text{m}$ was found to be $\sigma = 4.8 \times 10^{-18} \text{ cm}^2$. Using this cross section and using the 1.1 μm absorption length of our 485 nm pulse as the depth over

which the carriers are first distributed yields an initial carrier density of $n = \alpha/\sigma \approx 7 \times 10^{20} \text{ cm}^{-3}$. This number should be taken as a preliminary estimate since a 1.06 μm laser generates carriers with very little excess energy whereas our 485 nm laser inserts carrier pairs with an excess energy of $\sim 1.5 \text{ eV}$. The absorption cross section for very hot free carriers may be significantly different.

The principal conclusion of the transmission measurement is that there is no evidence of a molten silicon phase with absorption in any way approaching that of normal molten silicon with its skin depth of $\sim 100 \text{ \AA}$. An alternative explanation for the flat-topped enhanced reflectivity signal is the existence of a dense solid-state plasma. However the present data, like the results of Nathan, et. al.,¹¹ who failed to find a wavelength-dependent reflectivity duration, contradict the results expected from an ordinary Drude model of a simple plasma for the following reason: We obtained the usual flat-topped reflectivity behavior also at $\lambda_1 = 457.9 \text{ nm}$ which implies that the plasma frequency exceeds this blue laser frequency. Thus $\omega_p > \omega_L = 4.1 \times 10^{15} \text{ rad/sec}$. The Drude model of the electrons then predicts a skin depth which decreases with frequency below ω_p . Thus for a probe at $\lambda_2 = 1.15 \mu\text{m}$, one ought to see a skin depth for the light intensity given by

$$\delta = \frac{c}{2(\omega_p^2 - \omega_2^2)^{1/2}} > \frac{c}{2(\omega_1^2 - \omega_2^2)^{1/2}} = 400 \text{ \AA} \quad (1)$$

If the plasma exists to a depth of $\sim \alpha^{-1}$ of the 485 nm excitation pulse, ($\alpha^{-1} = 1.1 \mu\text{m}$) then severe attenuation of the 1.15 μm probe should occur. This is definitely not observed. Furthermore a plasma-like reflectivity at $\lambda = 457.9 \text{ nm}$ requires a density of

$$n = \frac{\omega_p^2}{4\pi e} \frac{m^* \epsilon(\infty)}{e} = 5 \times 10^{21} \text{ cm}^{-3} \quad (2)$$

with $\epsilon(\infty) = 1$ and $m^* = m_0$. (Since the electron system is very dense and presumably very hot the free electron mass, m_0 , seems a reasonable choice for m^* . The use of a high frequency dielectric constant of 1 is probably not reasonable but the effect of using larger values for $\epsilon(\infty)$ pushes n even higher.) This minimum density needed for explaining a plasma-like reflectivity is about an order of magnitude higher than our estimate based on free carrier absorption.

Recently Van Vechten and Wautelet¹² have calculated that there will be changes to the electronic energy band structure and a decrease of the band gap sufficient, possibly even to lead to plasma confinement at plasma densities in the low $10^{21}/\text{cm}^3$ range. Large shifts in the band structure would certainly produce changes in the optical reflectivity spectrum as well. If plasma confinement occurs this reflectivity change could appear flat-topped for a significant duration.

The Raman measurements of lattice temperature presented here appear to require the electronic system either to retain most of the absorbed laser energy for periods of tens of nanoseconds or to diffuse the energy over a distance significantly greater than 1 μm before releasing it to the lattice. Dense plasma effects are undoubtedly intimately related to the annealing

mechanisms with pulsed lasers and pulsed electron beams but much work remains before we obtain a completely satisfying understanding of the physics involved.

The authors would like to thank J. A. Van Vechten and R. T. Hodgson for stimulating conversations during the course of these experiments. The support of the Office of Naval Research (contract no. N000 14-80-C-0419) is gratefully acknowledged.

REFERENCES

1. I. B. Khaibullin, B. I. Shtyrkov, M. M. Zaripov, R. M. Bayazitov and M. F. Galjautdinov, *Radiation Effects* 36, 225 (1978).
2. P. Baeri, S. U. Campisano, G. Foti and E. Rimini, *Appl. Phys. Lett.* 32, 137 (1978); P. Baeri, S. U. Campisano, G. Foti and E. Rimini, *Phys. Rev. Lett.* 41, 1246 (1978); J. C. Wang, R. F. Wood, and P. R. Pronko, *Appl. Phys. Lett.* 33, 455 (1978); R. F. Wood, *Appl. Phys. Lett.* 37, 302 (1980); P. Baeri, S. U. Campisano, G. Foti and E. Rimini, *J. Appl. Phys.* 50, 788 (1979); J. R. Meyer, F. J. Bartoli and M. R. Kruer, *Phys. Rev. B* 21, 1559 (1980).
3. J. A. Van Vechten, R. Tsu, F. W. Saris and D. Hoonhout, *Phys. Lett.* 74a, 417 (1979); J. A. Van Vechten, R. Tsu and F. W. Saris, *Phys. Lett.* 74a, 422 (1979); J. A. Van Vechten, *J. de Phys.* 41 C-15 (1980) (Proceedings of the Mons Conference on Laser-Induced Nucleation in Solids, Mons, Belgium 4-6 Oct 1979.)
4. D. H. Auston, C. M. Surko, T. N. C. Venkatesan, R. E. Slusher and J. A. Golovchenko, *Appl. Phys. Lett.* 33, 437 (1978).
5. C. M. Surko, A. L. Simons, D. H. Auston, J. A. Golovchenko, R. E. Slusher and T. N. C. Venkatesan, *Appl. Phys. Lett.* 34, 635 (1979); D. H. Auston, J. A. Golovchenko, A. L. Simons, C. M. Surko and T. N. C. Venkatesan, *Appl. Phys. Lett.* 34, 363 (1979); Y. S. Lin and K. L. Wang, *Appl. Phys. Lett.* 34, 363 (1979); K. Murakami, M. Kawabe, K. Gamo, S. Namba and Y. Aoyagi, *Phys. Lett.* 70A, 332 (1979).
6. H. W. Lo and A. Compaan, *Appl. Phys. Lett.* (to be published).
7. H. W. Lo and A. Compaan, *Phys. Rev. Lett.* 44, 1604 (1980).
8. W. S. Johnson and J. F. Gibbons, Projected Range Statistics in Semiconductors (Standford U. P., Standford, 1969).
9. We are grateful to M. Gibson for performing the TEM studies.
10. W. B. Gauster and J. C. Bushnell, *J. Appl. Phys.* 41, 3850 (1970); J. P. Woerdman, *Philips Res. Repts. Suppl.* 7 (1971) p 1.
11. M. I. Nathan, R. T. Hodgson and E. J. Yoffa, *Appl. Phys. Lett.* 36, 512 (1980).
12. J. A. Van Vechten and M. Wautelet, Proc. 11th Int'l Conf. Defects and Radiation Effects in Semicond. (Oiso, Japan, Sept. 8-11, 1980) *Inst. Phys. Conf. Ser.* (to be published).